HARNESSING BACTERIAL BIOLOGICAL DENITRIFICATION WITH ZERO-VALENT IRON FOR THE SUSTAINABLE REMOVAL OF NITRATE IN WATER SOURCES

Matthew Kwon

Abstract

Nitrate contamination of water sources poses severe environmental and public health risks. Excess nitrogen affects 59.5 million people in the US, and 46% of streams are contaminated. Traditional nitrate removal technologies like reverse osmosis, ion exchange, and nanofiltration are costly and often inaccessible in underserved areas. This study investigates the use of zero-valent iron (ZVI) granules as a low-cost electron donor to support Betaproteobacteria-driven denitrification. ZVI's high reduction potential and cathodic hydrogen generation make it a sustainable substitute for industrial electron donors like methanol at 984% lower cost. In this two-month experiment, two media systems (Media-1 and Media-2) supported Betaproteobacteria and were supplemented with ZVI. Nitrate concentrations (~25 mg/L initial) were measured using Hach 353 N (PP) tests. Results showed a consistent nitrate reduction of 78.32%, with final concentrations well below the EPA threshold of 10 mg/L. Positive bacterial growth was observed across all growth periods, with clear signs of acclimatization and increasing metabolic efficiency over time. Additionally, a custom-designed shaker system maintained uniform bacterial suspension, improving reliability and consistency. This study presents ZVI-supported denitrification as a scalable, statistically significant ($p<0.0045$), and affordable solution to nitrate contamination.

Keywords: Nitrate contamination, Zero-valent iron, Biological denitrification, Betaproteobacteria, Water purification

1. Introduction

1.1 Nitrate contamination

Carbon, hydrogen, oxygen, nitrogen, and phosphorus are elements that compose most of life. Nitrogen gas (N_2), specifically, constitutes 78% of the air in the atmosphere. However, humans cannot use this form of nitrogen (Martínez-Dalmau et al., 2021, p. 1). Instead, nitrogen fixation must occur, typically through special nitrogen-fixing bacteria that live in the soil (Hill et al., 1980, p. 180).

Due to a slow natural rate of nitrogen fixation, it tends to be the most limiting factor for terrestrial plant growth (Martínez-Dalmau et al., 2021, p. 1). Thus, nitrogen is commonly used in fertilizer to increase crop yields (Wick et al., 2012, p. 180). Unfortunately, the high usage of nitrogen has detrimental environmental impacts. Runoff carries 80% of added nitrogen out of fields because it is water-soluble and does not bind to the soil well (Wurtsbaugh et al., 2019, p. 6; Velusamy et al., 2021, p. 3170). Excess nitrogen in ground and surface water is a significant pollutant, affecting 59.5 million people in the US (Kim, 2018, p. 1; Schechinger, 2021). The Environmental Protection Agency found that 41% of streams and 46% of rivers are overly nitrogen-contaminated (Wurtsbaugh et al., 2019, p. 3). Increased discharge and the accumulation of nitrate in water bodies cause eutrophication (McIsaac et al., 2001, p. 166). High nitrogen levels in aquatic ecosystems cause algal blooms, which decompose, deplete oxygen, and create hypoxic (oxygen-absent) conditions, leading to “dead zones.” Increased phytoplankton also blocks light for benthic vegetation. Nitrogen eutrophication may also lead to dangerous “red tide” blooms (Wurtsbaugh et al., 2019, p. 2). Excess nutrients, even without hypoxia, can transform lake, river, and coastal ecosystems, shifting the food web from a system driven by benthic microalgae and macrophyte production to one dominated by phytoplankton (Wurtsbaugh et al., 2019, p. 3).

The EPA establishes 10 mg/L as the maximum level of nitrate in water sources. The reaction between nitrites and amines can develop carcinogenic nitrosamines, leading to cancer (Kumar et al., 2020, p. 3). There is also a positive correlation between nitrate and increased infant mortality, nervous system defects, diabetes, spontaneous abortions, and respiratory tract infections. The most conclusive correlation between nitrite and a disease is with methemoglobinemia. Methemoglobin forms when the iron in hemoglobin becomes oxidized by nitrite. Methemoglobin can not bind with oxygen, leading to stupor and cerebral anoxia (Fewtrell, 2004, p. 1371).

1.2 Nitrate Treatment Techniques

Biological denitrification is a cost-efficient and environmentally friendly method to filter wastewater. This solution is bested suited for industrial waste plants, which have the largest concentrations of nitrate (Velusamy et al., 2021, p. 1371). Denitrification is a biological process performed by denitrifying bacteria, which use nitrate and nitrite as terminal electron acceptors in the absence of oxygen. Most denitrifying bacteria are heterotrophs requiring electron donors for growth. The process involves sequential enzymatic reductions: nitrate is converted to nitrite by nitrate reductases (encoded by nas, nar, or nap genes), nitrite to nitric oxide by nitrite

reductases (nirK or nirS genes), nitric oxide to nitrous oxide by nitric oxide reductase (nor gene), and finally, nitrous oxide to nitrogen gas by nitrous oxide reductase (nosZ gene) (Brozinčević et al., 2024, pp. 1-2).

Currently, the expense of carbon sources accounts for 50% of the biological denitrification process. Carbon sources are necessary electron donors for the ETC. Methanol is the most common option because of its lower prices and easy accessibility. However, there are three primary issues with using methanol (Brozinčević et al., 2024, p. 2). First, methylotrophs are inefficient in lower temperatures (Mokhayeri et al., 2006, p. 7). Second, methanol is highly toxic and reactive and should not be used for drinking water (Cherchi et al., 2009, p. 1). Third, the price of methanol is susceptible to changes in the market, making it an unreliable source.

1.3 Zero-Valent Iron

Using alternative sources like iron granules could significantly lower the cost of the process. Organic compounds, sulfur, and iron are possible options for electron donors. However, iron is both the cheapest and safest alternative (Kim, 2018, p. 2). Zero-valent iron (Fe^0) can easily oxidize in contact with water and oxygen, further fueling redox reactions by releasing electrons. The specific properties of ZVI allow it to be an efficient and continuous source of cathodic hydrogen (Till et al., 1998, p. 638). ZVI is far more likely to reduce with a reduction potential of E^0= -44V compared to ferrous iron (Fe^2) with a reduction potential of E^0= +77V (Galdames et al., 2020, p. 2; Johnson et al., 2012, p. 22). This means that ZVI is more likely to produce electrons in a solution and thus removes more nitrate than its ferrous iron counterpart. Furthermore, autotrophic denitrification removes nitrate more cleanly by leaving less waste sludge behind than their heterotrophic counterparts (Velusamy et al., 2021, p. 1366). This helps to cut down on costs and manual labor even more.

ZVI has been used in other projects as a reducing agent. For example, ZVI-packed permeable reactive barriers can also remediate chromate-contaminated groundwater. As water passes through the barrier, the highly toxic and carcinogenic Cr(VI) is converted into Cr(III), an essential nutrient for humans (De Flora et al., 1990, p. 162; Mertz, 1981, p. 1). Additionally, ZVI reduces explosives like 2,4,6-trinitrotoluene and hexahydro-1,3,5-trinitro-1,3,5-triazine in groundwater. These compounds are broken down into smaller molecules, such as NO_3^- and NH_4^+, which can be further treated through biological processes (Oh et al., 2003, p. 4280).

1.4 Hydrogenophilic Denitrification

$$Fe_0 + 2H_2O \rightarrow Fe^{2+} + H_2 + 2OH^-$$

Figure 1: The equation of zero-valent iron reduction in water to produce hydrogen gas.

$$2NO_3^- + 5H_2 \rightarrow N_2 + 4H_2O + 2OH^-$$

Figure 2: The equation for the reduction of nitrate using hydrogen gas to create nitrogen gas.

Anaerobic iron corrosion generates hydrogen gas by reducing protons, and this cathodic hydrogen can be utilized by denitrifying microbes (See Figure 1 and Figure 2). This approach may address the challenges commonly associated with hydrogen-based denitrification (Kim, 2018, p. 9). Hydrogen is an ideal electron donor for denitrifying bacteria (Till et al., 1998, p. 638). Furthermore, the reactants of hydrogen (N_2 and H_2O) are harmless. It also has a low biomass yield, allowing for a higher efficiency of denitrification (Kim, 2018, p. 10). The primary downside of H_2 is its dangerous explosive properties. Fortunately, the ZVI system is hypoxic and reduces hazards.

1.5 Objectives

The core hypothesis was to discover whether zero-valent iron granules could be used to facilitate the removal of nitrate in water sources. This is based on the idea that ZVI could serve as an electron donor to enhance the activity of nitrate-reducing bacteria. ZVI is known for its ability to participate in redox reactions. When combined with nitrate-reducing bacteria, it may provide an environment to reduce nitrate to nitrogen gas or other less harmful nitrogen compounds. The specific objectives of the study were:

1) To investigate whether bacteria cultures have the ability to reduce nitrate levels when in a ZVI-based system.
2) To determine whether the conditions in the system are viable for the bacteria cultures and to examine if the population within the bacteria colonies can grow.

2. Methods and Materials

2.1 Bacteria Culture Sourcing

Denitrifying seed cultures were obtained from the activated sludge aeration basin of the Wilmington Wastewater Treatment Plant in Delaware. There is not a single species of bacteria within the basin, but rather tens of different species. Typically, the main phylum of bacteria found in the aeration basin is Proteobacteria, with the class Betaproteobacteria being particularly prevalent (Kim, 2018, p. 24). The richness of microbial diversity ensures the resilience and adaptability of the ecosystem to changing environmental conditions and nutrient loads.

2.2 Media Preparation

Figure 3: Glove box pumped with N_2 gas to prevent contact with oxygen. Old media bottle, new media bottle, and waste disposal bottle.

A 1000 mL glass bottle was first filled with water. The following chemicals were added to make the media. $NaHCO_3$ (600 mg/L) acted as a buffering agent to maintain optimal pH (Abdulkarim & Abdullahi, 2010, p. 981). KH_2PO_4 (600 mg/L) was a buffer and fulfilled the requirements for K and P elements (Mokhtari-Hosseini et al., 2009, p. 49). $MgCl_2$ (400 mg/L) and $MgSO_4$ (50 mg/L) supplied magnesium, crucial for the development of biofilm for bacteria cultures (Wang et al., 2019, p. 959). $CaCl_2$ (25 mg/L) was important structurally for the outer lipopolysaccharide layer and cell walls (Das et al., 2014, p. 1).

A trace element solution was used in bacterial growth media to provide essential micronutrients and minerals that are required in tiny amounts for the growth, metabolism, and physiological functions of bacteria. The formula for the trace element solution is the following. $FeCl_2$ (450 mg/L) provides iron which is crucial for electron transport and enzyme function (Wang et al., 2020, p. 1; *Iron Enzymes*, n.d.). $CoCl_2$ (190 mg/L) was used to create hypoxic conditions (Muñoz-Sánchez & Chánez-Cárdenas, 2018, p. 1). $MnSO_4$ (100 mg/L) helped with oxidative stress protection (Aguirre & Culotta, 2012, p. 13541). $ZnCl_2$ (52 mg/L) provided zinc, a

trace element found in many proteins and enzymes (Hantke, 2005, p. 196). Na_2MoO_4 (36 mg/L): Molybdenum acted as an enzyme to transfer electrons for nitrate reduction (Vega et al., 1971, p. 294). H_3BO_3 (30 mg/L): Boric acid helped to buffer the pH (Lopalco et al., 2020, p. 2375). $CuCl_2$ (29 mg/L) provided copper, a cofactor for nitrite reductase enzymes (Horrell et al., 2017, p. 1470). NiCl (24 mg/L) added nickel, significantly increasing nitrate reductase activity (Matraszek, 2008, p. 361). A 1 mL trace element solution was added per 1 L of media. Two bacterial systems were created: Media-1 and Media-2. Both media were identical in composition and underwent the same processes throughout the entire experiment.

The media needed to be replaced biweekly. To do so, a glove chamber was pumped with N_2 gas for at least 15 minutes (See Figure 3). All of the following steps occurred within the glove chamber to maintain anaerobic conditions. The media was carefully replaced with the new media, and 1 ml of trace element solution was added.

2.3 Experimental Conditions

Figure 4: Media shaker contraption to keep bacteria suspended.

The seed cultures were prepared by mixing activated sludge and anaerobic digester samples. The final biomass concentration was adjusted to approximately 1,000 mg/L TSS. Once the bacteria were in the bottle, they were left on a platform shaker configuration at 150 rpm (See Figure 4). The caps must be shut tight to prevent prolonged open-air contamination, as a reaction between hydrogen gas and oxygen could be explosive. The bottles were kept at 36 °C in a light-excluded chamber.

2.4 Analytical Procedure

Figure 5: Furnace used to incinerate organic content and determine mass.

Figure 6: Hach machine to measure nitrate.

Approximately 0.07 g of $NaNO_3$ was added daily, with more added if the following days were missed. $NaNO_3$ was used instead because it is highly soluble and provides a stable source of nitrate ions (NO_3^-) in aqueous solutions (Reynolds, 2018, p. 15150). Pure nitrate ions are not available as a stand-alone compound but rather as part of ionic salts like $NaNO_3$ or KNO_3. Sodium ions are less likely to interfere with the bacteria's metabolic processes compared to other cations like potassium or ammonium, making it a preferred choice for nitrate supplementation. Finally, sodium nitrate is easy to weigh, dissolve, and handle in the laboratory.

After adding the nitrate, volatile suspended solids (VSS) were measured to track bacterial growth. A 10 mL sample was collected with a pipette and filtered through a fiberglass filter connected to a vacuum pump. The filter was then put onto an aluminum weighing dish and weighed. The weighing dish was put into a furnace at 550 °C for 30 minutes, during which the

organic material was volatilized and lost (See Figure 5). The mass lost during incineration represents the organic fraction or volatile suspended solids (VSS). These samples were taken in duplicates to reduce statistical anomalies. Finding the volatile suspended solids is important to track bacterial growth because it provides a quantifiable measure of biomass concentration in the sample.

The Hach 353 N (PP) test was employed to analyze the nitrate content of the bacteria sample. This test operates through a colorimetric reaction, where the presence of nitrates in the sample triggers a chemical reaction with the reagents, producing a color change proportional to the nitrate concentration (See Figure 6). The resulting color intensity is then measured by a photometric device to determine the nitrate levels accurately. To conduct the test, the reagents were added to the sample, and the sample was shaken for 1 minute. After the initial reaction time, a 5-minute timer was started, during which an amber color would develop if nitrates were present. Simultaneously, a blank was prepared by filling another sample cell with 10 mL of the sample. When the 5-minute timer expired, the blank sample cell was cleaned and inserted into the instrument. Next, the prepared sample cell was inserted into the instrument within 2 minutes after the timer expired to complete the test.

3. Results

3.1 Nitrate Input

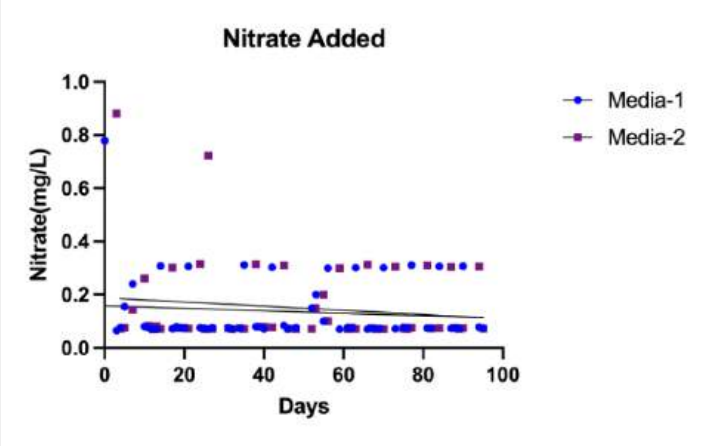

Figure 7: Nitrate added over time. No significant difference was observed (p = 0.6168), supporting comparable baseline conditions.

Media-1 and Media-2 experienced no statistical difference in nitrate addition. Media-1 had a mean of 0.1369 g and a median of 0.0765 g, while Media-2 showed a higher mean of 0.1503 g and a median of 0.0750 g. The two sets also had no statistically significant difference (p-value of 0.6168). The higher mean was due to an excess of nitrate added on weekends when the lab was closed. Similar variability and central tendencies suggest that both media received a similar amount of nitrate, establishing a baseline to view data extrapolation equally between the two media. Figure 7 displays the nitrate added over the course of the experiment.

3.2 Nitrate Reduction

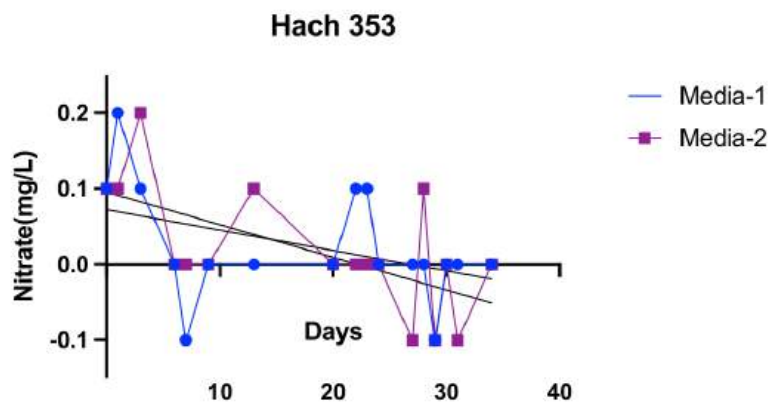

Figure 8: Nitrate levels over time. Both showed strong nitrate removal, with values near zero and decreasing trends, indicating increasing bacterial efficiency.

Bacteria in both Media-1 and Media-2 exhibited a similar capability to remove nitrate, as seen by the Hach 353 N (PP) tests that were conducted (See Figure 8). A mode of 0 (12 occurrences) highlighted low nitrate levels, suggesting bacteria consume nearly all nitrate. The mean (0.04375) and median (0) further indicate a similar conclusion. Negative values appeared

5 times in the 32 samples due to very low nitrate levels. Excluding negatives yielded a similar average (0.0444) and the same median, confirming the prior conclusion. These values fall well below the EPA's 10 mg/L threshold. Media-1 and Media-2 had slopes of -0.00269 and -0.00431, respectively. This indicates that the bacteria became more efficient at denitrification as time progressed. The bacteria likely became more accustomed to their systems.

3.3 Bacterial Growth

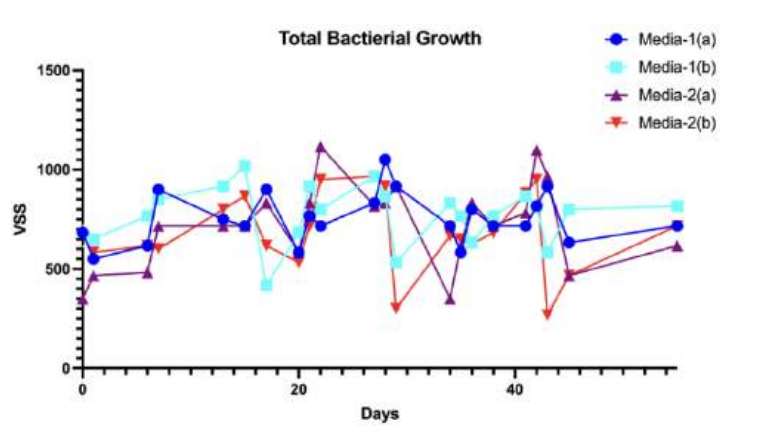

Figure 9: The graph shows the comprehensive bacterial growth through VSS over the experiment.

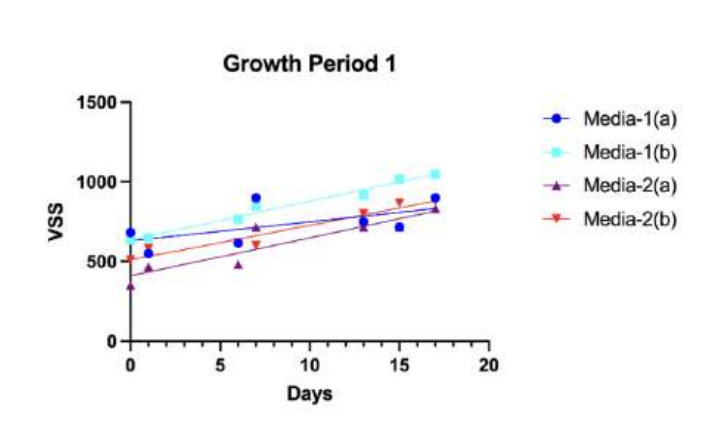

Figure 10: GP1 growth trends in all media. Three of four datasets showed statistically significant positive growth with strong model fits ($R^2 > 0.83$).

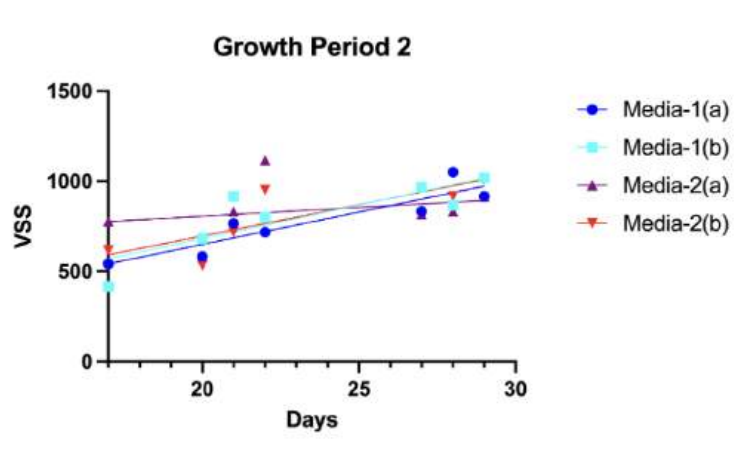

Figure 11: The graph shows the VSS of the bacterial media during Growth Period 2 (GP2).

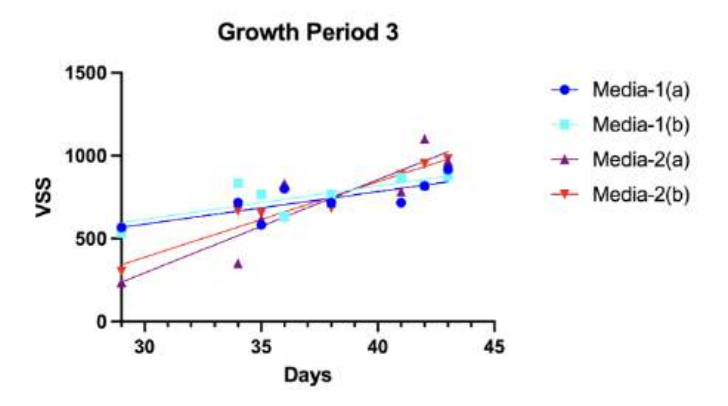

Figure 12: GP3 showed positive growth in all datasets, with Media-2(a) and Media-2(b) exhibiting statistically significant trends and strong model fits in particular.

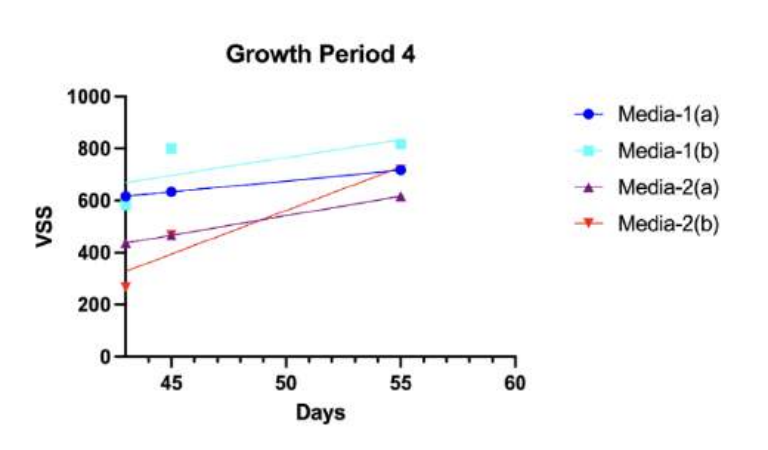

Figure 13: GP4 demonstrated consistent positive growth across all datasets, with strongest model fits in Media-1(a) and Media-2(a) ($R^2 = 1$), though only partial statistical significance was observed.

Media-1 and Media-2 repeatedly displayed the ability to repopulate . Bacterial growth, measured by volatile suspended solids (VSS), showed positive trends across all growth periods

(GP): GP1 [7/2/24(a)-7/19(a)], GP2 [7/19(b)-7/31(a)], GP3 [7/31(b)-8/14(a)], GP4 [8/14(b)-8/27(b)] (See Figure 9. Since bacteria populations reset every time the media was replaced, each period was analyzed individually. The VSS (mg/L) were taken in duplicates (signified by a and b) to reduce outliers. Due to this, the data was analyzed separately as they were taken on the same day. Furthermore, the data was examined by growth period rather than their entire experimental time to develop a comprehensive and holistic picture.

GP1 demonstrated consistent positive growth across all four data sets, as evidenced by statistical analyses (See Figure 10). The mean values for Media-1(a), Media-1(b), Media-2(a), and Media-2(b) were 11.86, 24.27, 23.97, and 21.72, respectively, indicating strong upward trends. Notably, three of the four data sets (Media-1(b), Media-2(a), and Media-2(b)) showed significant deviations from zero, confirmed by their respective p-values (0.0045, 0.0043, and 0.018). The R^2 values further underscored the reliability of the models, with Media-1(b) achieving the highest value at 0.9521, followed by Media-2(b) at 0.8814 and Media-2(a) at 0.83, indicating that the data points followed the regression line. Additionally, the 95% confidence bands for Media-1 b (14.27 to 34.26), Media-2(a) (11.50 to 36.45), and Media-2(b) (7.081 to 36.37) demonstrated strong intervals of positive growth, whereas Media-1(a)'s confidence band (-6.261 to 29.99) suggested potential variability. Overall, these results highlighted GP1's significant and reliable growth across the examined metrics, particularly in the three data sets where statistical significance was observed.

GP2 exhibited positive growth across all four data sets, with statistical measures varying between media types (See Figure 11). The mean values ranged from 9.677 (Media-2(a)) to 37.34 (Media-1(a)), indicating unanimous growth. While Media-1(a) and Media-1(b) showed positive deviation from zero, Media-2(a) and Media-2(a) did not, suggesting differing degrees of consistency or effect. R^2 values highlighted the strength of the fit of the data for Media-1(a), Media-1(b), and Media-2(b) (0.7603, 0.6157, and 0.6241). The p-value for Media-1(a) ($p = 0.0236$) was statistically significant, indicating a meaningful effect. The p-values for the other data sets ($p = 0.0646$ and $p = 0.0615$ for Media-1(b) and Media-2(b)) approached significance but did not meet the conventional threshold ($p = 0.05$). The 95% confidence bands reflected variability, with narrower ranges in Media-1(a) (7.917 to 63.91) and broader intervals in Media-2 a (-49.55 to 68.91), further emphasizing the differences in data reliability and precision. These findings collectively suggest that Media-1 conditions provided stronger and more consistent evidence of positive growth compared to Media-2 conditions.

GP3 revealed positive growth across all four data sets, as evidenced by the statistical analysis (See Figure 12). The means for Media-1(a), Media-1(b), Media-2(a), and Media-2(b) were 19.64, 20.09, 56.19, and 45.53, respectively, demonstrating an upward trend in performance metrics. Notably, Media-2(a) and Media-2(b) showed significant deviation from zero, suggesting meaningful growth in these data sets. The R^2 values further reinforced the reliability of these trends, increasing progressively from Media-1(a) to Media-2(b) (0.4555, 0.5525, 0.6922, and 0.9295), indicating a strong model fit. The p-values corroborated these findings, with Media-1(b) ($p = 0.0555$), Media-2(a) ($p = 0.0203$), and Media-2(b) ($p = 0.0005$),

highlighting the robustness of these results. Additionally, the 95% confidence bands for Media-2(a) (13.12 to 99.26) and Media-2(b) (31.12 to 59.95) affirmed the precision of these estimates, showing narrower and more positive ranges compared to Media-1(a) and Media-1(b). Collectively, these metrics demonstrated substantial and statistically significant growth for GP3, particularly in the Media-2 datasets.

As reflected in key statistical measures, GP4 exhibited consistent positive growth across all four data sets (See Figure 13). For Media-1(a) and Media-2(a), the mean values were 8.333 and 15, respectively, with perfect R^2 values of 1, indicating a strong fit of the model to the data. For Media-1(b) and Media-2(b), the mean values were 13.71 and 33.47, respectively, accompanied by R^2 values of 0.4585 and 0.9108, suggesting varying levels of model strength. Despite these differences, the deviation from zero was not statistically significant for either Media-1(b) or Media-2(b), as evidenced by their p-values of 0.5265 and 0.1931, both above the typical significance threshold of 0.05. These metrics collectively underscored GP4's robust growth trajectory while acknowledging statistical variability in some cases. Notably, GP4 was also the shortest growing period.

4. Discussion

4.1 Discussion of Results

The results of this study demonstrated that ZVI can act as an effective electron donor for denitrifying bacteria. Over the experimental period, both Media-1 and Media-2 systems showed consistent nitrate reduction trends. Several statistical measurements helped to allude to this conclusion. The mean amount of nitrate was close to zero (0.04375), and 17 of 32 samples recorded values of zero or less. The EPA declares anything over 10 mg/L of nitrate as contaminated. Thus, the experiment was effective in this regard. Furthermore, the negative slopes in Media-1 (–0.00269) and Media-2 (–0.00431) show promise that the systems support bacterial acclimatization. This would be important as it would allow for a real-world ZVI-based denitrification system to be viable in the long term.

The analysis of bacterial culture growth also revealed the population's strength and resilience. After replacing the medium biweekly, the bacteria populations were always able to recuperate. Every subset (Media-1(a), Media-1(b), Media-2(a), and Media-2(b)) showed positive growth during every growth period. This highlights the compatibility between the denitrifying bacteria and the ZVI systems. Additionally, it displayed that the solutions for media and trace elements were viable designs.

Moreover, the consistent trend between Media-1 and Media-2 in denitrification and bacterial growth is important. They indicate that the process is not only reproducible but also adaptable to different configurations or environmental conditions. This is a critical factor when considering scalability and practical implementation in real-world scenarios. In conclusion, the results of this study provide compelling evidence that ZVI is a reliable and sustainable electron donor for denitrifying bacteria.

4.2 Bacterial Acclimitization

Bacterial acclimatization is a crucial process in which microbial communities adapt to environmental conditions, optimizing their metabolic activity over time. Throughout the experiment, Media-1 and Media-2 had negative slopes in their recorded level of nitrate (-0.00269 and -0.00431). Meanwhile, Media-1 and Media-2 both had an increased rate of nitrate removal (0.0726 and 0.0782). Notably, these trends emerged despite constant experimental conditions, underscoring the adaptive capabilities of the bacterial cultures in response to ZVI. These findings highlight the potential of ZVI in enhancing bacterial denitrification by facilitating microbial acclimatization and improving nitrate reduction rates. The observed efficiency gains suggest that incorporating ZVI into bioremediation strategies could optimize nitrate removal in contaminated water systems. Future research should explore long-term bacterial adaptations and potential synergistic effects between ZVI and different microbial communities to further refine denitrification processes.

4.3 Comparative Analysis

ZVI is significantly more cost-effective and efficient than the alternative electron donor of methanol. ZVI is 9984% cheaper and 10^6 more efficient per gram. Methanol has the added

downside of being both toxic in large quantities and price-volatile. Furthermore, heterotrophic denitrification produces less biowaste sludge.

4.4 Future Work

Several factors could have influenced the results. One significant limitation was the variability in nitrate addition due to logistical constraints on weekends. Although this variability was statistically insignificant (p-value of 0.6168), it could have introduced minor inconsistencies in bacterial adaptation processes.

Future studies should consider increasing the number of replicates and incorporating more varied experimental conditions to enhance the robustness of the findings. For example, testing different ZVI particle sizes or concentrations could clarify the optimal conditions for nitrate removal. A larger surface area may be more efficient at denitrification, but it may also push the system's pH to unviable conditions (Till et al., 1998, p. 638)

Additionally, employing advanced analytical techniques to monitor intermediate nitrogen compounds, such as nitrite and ammonium, would help clarify the denitrification pathway. The introduction of complementary processes, like anammox, to mitigate ammonium accumulation should also be explored. This approach could integrate anammox bacteria with ZVI systems, potentially improving nitrogen removal efficiency while minimizing undesirable byproducts.

References

1. Abdulkarim, Bala Isah, and Mohammed Evuti Abdullahi. "Effect of Buffer (NaHCO3) and Waste Type in High Solid Thermophilic Anaerobic Digestion." *International Journal of ChemTech Research*, vol. 2, no. 2, June 2010, pp. 980-84. *Sphinx Knowledge House*, sphinxsai.com/s_v2_n2/CT_V.2No.2/ChemTech_Vol_2No.2_pdf/C%20T=36%20(980-984).pdf. Accessed 2 Dec. 2024.
2. Aguirre, J. Dafhne, and Valeria C. Culotta. "Battles with Iron: Manganese in Oxidative Stress Protection." *Journal of Biological Chemistry*, vol. 287, no. 17, Apr. 2012, pp. 13541-48. *Journal of Biological Chemistry*, https://doi.org/10.1074/jbc.r111.312181. Accessed 2 Dec. 2024.
3. Brozinčević, Andrijana, et al. "Cost Reduction in the Process of Biological Denitrification by Choosing Traditional or Alternative Carbon Sources." *Energies*, vol. 17, no. 15, 25 July 2024, p. 3660. *Multidisciplinary Digital Publishing Institute*, https://doi.org/10.3390/en17153660. Accessed 27 Nov. 2024.
4. Cherchi, Carla, et al. "Implication of Using Different Carbon Sources for Denitrification in Wastewater Treatments." *Water Environment Research*, vol. 81, no. 8, Aug. 2009, pp. 788-99. *PubMed*, https://doi.org/10.2175/106143009x12465435982610. Accessed 25 Dec. 2024.
5. Das, Theerthankar, et al. "Influence of Calcium in Extracellular DNA Mediated Bacterial Aggregation and Biofilm Formation." *PLOS ONE*, vol. 9, no. 3, 20 Mar. 2014. *PLOS ONE*, https://doi.org/10.1371/journal.pone.0091935. Accessed 2 Dec. 2024.
6. De Flora, Silvio, et al. "Genotoxicity of Chromium Compounds. a Review." *Mutation Research/Reviews in Genetic Toxicology*, vol. 238, no. 2, Mar. 1990, pp. 99-172. *PubMed*, https://doi.org/10.1016/0165-1110(90)90007-x. Accessed 25 Dec. 2024.
7. Fewtrell, Lorna. "Drinking-Water Nitrate, Methemoglobinemia, and Global Burden of Disease: A Discussion." *Environmental Health Perspectives*, vol. 112, no. 14, Oct. 2004, pp. 1371-74. *Environmental Health Perspectives*, https://doi.org/10.1289/ehp.7216. Accessed 26 Nov. 2024.
8. Galdames, Alazne, et al. "Zero-Valent Iron Nanoparticles for Soil and Groundwater Remediation." *International Journal of Environmental Research and Public Health*, vol. 17, no. 16, 11 Aug. 2020, p. 5817. *National Institute of Health*, https://doi.org/10.3390/ijerph17165817. Accessed 28 Nov. 2024.
9. Hantke, Klaus. "Bacterial Zinc Uptake and Regulators." *Current Opinion in Microbiology*, vol. 8, no. 2, Apr. 2005, pp. 196-202. *ScienceDirect*, https://doi.org/10.1016/j.mib.2005.02.001. Accessed 2 Dec. 2024.
10. Hill, R. D., et al. "Atmospheric Nitrogen Fixation by Lightning." *Journal of the Atmospheric Sciences*, vol. 37, no. 1, Jan. 1980, pp. 179-92. *American Meteorological Society*, journals.ametsoc.org/view/journals/atsc/37/1/1520-0469_1980_037_0179_anfbl_2_0_co_2.xml.

11. Horrell, Sam, et al. "Recent Structural Insights into the Function of Copper Nitrite Reductases." *Metallomics*, vol. 9, no. 11, 2017, pp. 1470-82. *Oxford Academic*, https://doi.org/10.1039/c7mt00146k. Accessed 2 Dec. 2024.
12. "Iron Enzymes." *ScienceDirect*, Elsevier, www.sciencedirect.com/topics/biochemistry-genetics-and-molecular-biology/iron-enzymes#:~:text=Iron%20is%20the%20third%20most,%2Dsulfur%20clusters%20%5B40%5D. Accessed 2 Dec. 2024.
13. Johnson, D. Barrie, et al. "Redox Transformations of Iron at Extremely Low PH: Fundamental and Applied Aspects." *Frontiers in Microbiology*, vol. 3, 2012. *PubMed*, https://doi.org/10.3389/fmicb.2012.00096. Accessed 28 Nov. 2024.
14. Kim, Inyoung. "Denitrification by Zero-Valent Iron-Supported Mixed Cultures." *Doctoral Dissertations (Winter 2014 to Present)*, 2018. *University of Delaware*, udspace.udel.edu/items/454d7661-f201-4faf-9992-6cdf909547aa. Accessed 26 Nov. 2024.
15. Kumar, Pavitra, et al. "Review of Nitrogen Compounds Prediction in Water Bodies Using Artificial Neural Networks and Other Models." *Sustainability*, vol. 12, no. 11, 26 May 2020. *Multidisciplinary Digital Publishing Institute*, https://doi.org/10.3390/su12114359. Accessed 26 Nov. 2024.
16. Lopalco, Antonio, et al. "Boric Acid, a Lewis Acid with Unique and Unusual Properties: Formulation Implications." *Journal of Pharmaceutical Sciences*, vol. 109, no. 8, Aug. 2020, pp. 2375-86. *ScienceDirect*, https://doi.org/10.1016/j.xphs.2020.04.015.
17. Martínez-Dalmau, J., Berbel, J., & Ordóñez-Fernández, R. (2021). Nitrogen fertilization. A review of the risks associated with the inefficiency of its use and policy responses. *Sustainability*, *13*(10). https://doi.org/10.3390/su13105625
18. Matraszek, Renata. "Nitrate Reductase Activity of Two Leafy Vegetables as Affected by Nickel and Different Nitrogen Forms." *Acta Physiologiae Plantarum*, vol. 30, no. 3, 10 Jan. 2008, pp. 361-70. *Springer Nature*, https://doi.org/10.1007/s11738-007-0131-5. Accessed 2 Dec. 2024.
19. McIsaac, G. F., David, M. B., Gertner, G. Z., & Goolsby, D. A. (2001). Nitrate flux in the mississippi river. *Nature*, *414*(6860), 166-167. https://doi.org/10.1038/35102672
20. Mertz, Walter. "The Essential Trace Elements." *Science*, vol. 213, no. 4514, 18 Sept. 1981, pp. 1332-38. *PubMed*, https://doi.org/10.1126/science.7022654. Accessed 25 Dec. 2024.
21. Mokhayeri, Y., et al. "Examining the Influence of Substrates and Temperature on Maximum Specific Growth Rate of Denitrifiers." *Water Science and Technology*, vol. 54, no. 8, 1 Oct. 2006, pp. 155-62. *PubMed*, https://doi.org/10.2166/wst.2006.854. Accessed 25 Dec. 2024.
22. Mokhtari-Hosseini, Zahra B., et al. "Media selection for poly (hydroxybutyrate) production from methanol by Methylobacterium extorquens DSMZ 1340." *Iranian Journal of Chemistry and Chemical Engineering*, vol. 28, no. 3, 2009, pp. 45-52. *Academic Jihad*

Scientific Information Center Database, www.sid.ir/EN/VEWSSID/J_pdf/84320095102.pdf. Accessed 2 Dec. 2024.
23. Muñoz-Sánchez, Jorge, and María E. Chánez-Cárdenas. "The Use of Cobalt Chloride as a Chemical Hypoxia Model." *Journal of Applied Toxicology*, vol. 39, no. 4, 28 Nov. 2018, pp. 556-70. *Wiley*, https://doi.org/10.1002/jat.3749. Accessed 2 Dec. 2024.
24. Oh, Seok-Young, et al. "Enhancing Fenton Oxidation of TNT and RDX through Pretreatment with Zero-valent Iron." *Water Research*, vol. 37, no. 17, Oct. 2003, pp. 4275-83. *PubMed*, https://doi.org/10.1016/s0043-1354(03)00343-9. Accessed 25 Dec. 2024.
25. Reynolds, Jacob G. "Salt Solubilities in Aqueous Solutions of NaNO3, NaNO2, NaCl, and NaOH: A Hofmeister-like Series for Understanding Alkaline Nuclear Waste." *ACS Omega*, vol. 3, no. 11, 9 Nov. 2018, pp. 15149-57. *American Chemical Society Publications*, https://doi.org/10.1021/acsomega.8b02052. Accessed 3 Dec. 2024.
26. Schechinger, Anne. "Nitrate contaminates drinking water for almost 60 million people in cities across the country." *Environmental Working Group*, 3 Nov. 2021, www.ewg.org/tapwater/nitrate-contaminates-drinking-water.php. Accessed 27 Nov. 2024.
27. Till, Brian A., et al. "Fe(0)-Supported Autotrophic Denitrification." *Environmental Science & Technology*, vol. 32, no. 5, 22 Jan. 1998, pp. 634-39. *American Chemical Society*, https://doi.org/10.1021/es9707769. Accessed 25 Dec. 2024.
28. Vega, J. MA, et al. "Role of Molybdenum in Nitrate Reduction by Chlorella." *Plant Physiology*, vol. 48, no. 3, 1 Sept. 1971, pp. 294-99. *Oxford Academic*, https://doi.org/10.1104/pp.48.3.294. Accessed 2 Dec. 2024.
29. Velusamy, Karthik, et al. "Advanced Techniques to Remove Phosphates and Nitrates from Waters: A Review." *Environmental Chemistry Letters*, vol. 19, no. 4, 13 Apr. 2021, pp. 3165-80. *Springer Nature*, https://doi.org/10.1007/s10311-021-01239-2. Accessed 27 Nov. 2024.
30. Wang, Ru, et al. "Iron as Electron Donor for Denitrification: The Efficiency, Toxicity and Mechanism." *Ecotoxicology and Environmental Safety*, vol. 194, May 2020. *ScienceDirect*, https://doi.org/10.1016/j.ecoenv.2020.110343. Accessed 2 Dec. 2024.
31. Wang, Tianyang, et al. "Magnesium and Calcium Ions: Roles in Bacterial Cell Attachment and Biofilm Structure Maturation." *Biofouling*, vol. 35, no. 9, 21 Oct. 2019, pp. 959-74. *Taylor & Francis Online*, https://doi.org/10.1080/08927014.2019.1674811.
32. Wick, Katharina, et al. "Groundwater nitrate contamination: Factors and indicators." *Journal of Environmental Management*. *ScienceDirect*, https://doi.org/10.1016/j.jenvman.2012.06.030. Accessed 26 Nov. 2024. Originally published in *Journal of Environmental Management*, vol. 111, 30 Nov. 2012, pp. 178-86.
33. Wurtsbaugh, Wayne A., et al. "Nutrients, eutrophication and harmful algal blooms along the freshwater to marine continuum." *WIREs Water*, vol. 6, no. 5, Sept.-Oct. 2019. *Wiley Interdisciplinary Reviews*, https://doi.org/10.1002/wat2.1373. Accessed 26 Nov. 2024.